Development of an Imaging Spectrometer for High-Repetition Rate Proton Measurement

Contact: matthew.alderton@strath.ac.uk

M. Alderton, R. Wilson, T. P. Frazer, E. J. Dolier, J. Patel, M. Peat, E. F. J. Bacon, R. J. Gray and P. McKenna
Department of Physics
University of Strathclyde,
Glasgow, United Kingdom,
G4 0NG

S. Astbury, T. Dzelzainis, O. Finlay, C. Armstrong and C. Spindloe
Central Laser Facility
Rutherford Appleton Laboratory,
Didcot, United Kingdom,
OX11 0QX

Abstract

As laser-driven proton sources increase in repetition-rate to match upcoming laser facilities, new and improved diagnostics will be required to measure the spatial and spectral profiles of laser-driven proton beams as current proton measurement technologies are incompatible with high-repetition rate operation. In this report, we present development of an imaging spectrometer using Lanex as an active detector to simultaneously measure the spatial and spectral profile of laser-driven proton beams, based on a 3D printed step filters.

1 Introduction

With the advent of high repetition-rate laser facilities the ability to directly measure accelerated particles generated in laser-plasma interactions at the laser repetition-rate is vital to allow the use of parameter searching mechanisms and experimental optimisation routines [1, 2]. Existing proton diagnostics are typically unable to simultaneously measure the spatial and spectral profiles of the proton beam at high repetition-rate. The Thomson parabola samples part of the proton beam and uses perpendicular magnetic and electric fields to disperse charged particles according to their charge-to-mass ratio. This results in a high-resolution measurement of the spectral profile of the generated proton beam and can be operated in conjunction with an MCP to operate at high repetition-rate. In spite of these benefits the Thomson Parabola does not measure the spatial profile of the beam and for non-uniform beams. for example the spatial profile shown in Higginson *et al.* [3] which shows a peak dose at and angle between the target normal and laser axis. A Thomson measurement of this beam could lead to a misrepresentation of the proton spectrum. The standard for spatial measurement of proton beams is the Radiochromic Film stack (RCF stack), which uses layers of filtering material and layers of Radiochromic Film to measure the spatial profile of the beam at varying energies throughout the stack according to the proton stopping power required to reach each layer of detector in the stack. This builds a clear picture of the spatial profile of the beam for a range of energies but this device is a single use diagnostic, with the proton beam captured by irreversibly colouring the RCF. As a result this is incompatible with high repetition-rate experiments. In a similar vein active footprint monitors have been used to measure the spatial profile of a beam using scintillating devices capable at operating at high repetition-rate, however these typically only sample a small number of proton energies (up to three) and thus this device favours a high spatial resolution with a limited spectral resolution [4].

The PROBIES (Proton Beam Imaging Energy Spectrometer) concept is a proton measurement device developed by Mariscal *et al.*, at the Lawrence Livermore National Laboratory (LLNL) [5, 6]. In this concept a block of peaks of varying thickness of material is repeated across a square to form the PROBIES mask. Each thickness of peak in the block will require a different minimum energy proton to pass through the peak and reach the detector on the rear side. With this block repeated in a grid pattern the proton beam can be uniformly sampled at regular intervals for each of the energies associated with the peaks in the block. Once sampled, each of the energy bins can be interpolated to reconstruct the beam profile between peaks, giving a spatial measurement of the proton beam for each of the energies in the block. Whilst this concept has been demonstrated as a tool for high-resolution RCF measurements and online scintillation based measurement it has not been demonstrated in a high repetition-rate environment. We aim to build on previous work to develop the system so that it can be used for instant proton spectrum measurement, initially at the 1 Hz rate before progressing to 10 Hz.

2 Mask Design

The spectrometer mask designed with a repeating block of 9 peaks. In this mask each peak had a transverse size of 1 mm and with the 9 peaks in the block equate to 9 spectral points in a total space of a 3×3 mm square. A uniform array of 12×12 of these blocks were arranged to form a 36 mm square detector area. A slot of 8×2 blocks of peaks was removed from the centre of the

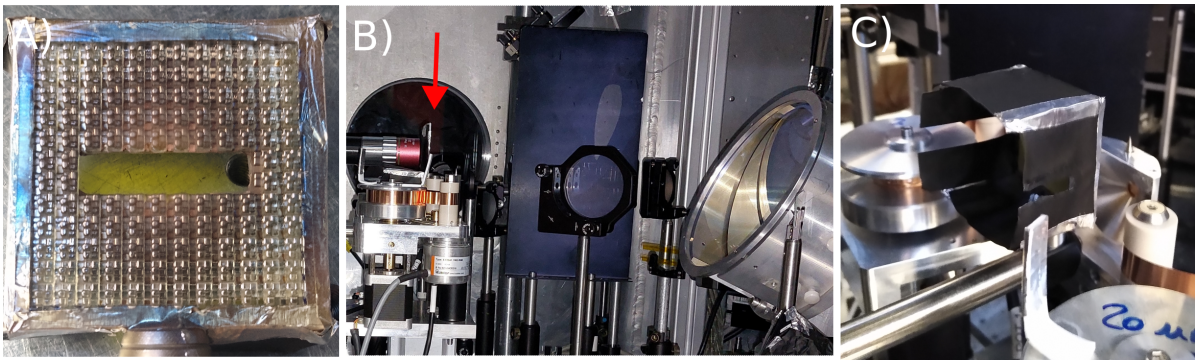

Figure 1: A) The 3D printed PROBIES mask front surface. The device contains an active surface of 36 mm with the Lanex scintillator attached to the rear of the mask. B) The experimental setup used to test the device. The red arrow indicates the location of the PROBIES device, between the spools of the tape target. C) The PROBIES device behind the tape target, note the vertical offset between the detector and target is due to the target shown in the 'out' position.

mask to maintain line of sight to the target to enable use of additional diagnostics in parallel with the proton detector. An example of the 3D printed mask for the front of this detector can be seen in FIG. 1 A). The mask was backed with a 13 um layer of aluminium to block heavy ions and a sheet of Lanex was affixed to the back of the mask to convert the proton dose into visible light for use as an active detector. These masks were designed to be 3D printed. This allowed rapid, cost-effective development of masks and allowed the design to be varied day to day. The masks were printed using a proprietary plastic with density of ≈ 1.17 gcm^{-3}. SRIM modelling was used to determine the material heights necessary for the individual peaks in the block to sample a range of proton energies from 1-22 based on the plastic density.

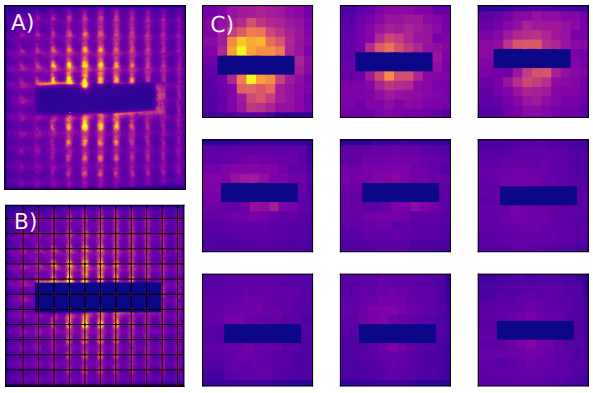

Figure 2: A) Raw image collected from the fibre bundle imaging setup. B) Image from the mask rear after peak location and blocking of the mask slit. C) Interpolation of the spatial profiles of each peak in the mask design. Peak breakthrough energy increases from left to right.

3 Experimental Methods

The proton spectrometer was tested using the Astra-Gemini laser in TA3. Pulses of p-pol light of central wavelength 810 nm with a pulse duration of 40 fs delivered up to 5.3 J of energy on target. The beam was focused using an f/2 off-axis parabola into a nominal best focus spot size of 3 μm on a 15 μm thick copper tape target [7]. A dual plasma mirror system was deployed to boost the temporal-intensity contrast and the south beam was employed as a pre-heater beam to control the front surface plasma scale length. Protons and ions were accelerated from the target rear via target normal sheath acceleration [8] with radiochromic film measurements indicating maximum observed proton energies of up to 22 MeV.

The proton spectrometer was placed in the same position as a typical RCF stack, approximately 40 mm behind the target as shown in FIG. 1 B) and C). The emitting surface of the lanex was imaged using a folding mirror to locate the lens off-axis with the image then relayed out of the target chamber using a fibre bundle. Suitable bandpass filtering was applied to ensure only scintillation signal from the Lanex was collected. The image was relayed onto an Andor Neo CCD outside of the target chamber.

4 Analysis and Results

Once raw images were captured the peaks on the image were defined. Fiducial markers on the mask rear pointed to the lowest energy peaks and grid lines were mapped to these peaks. Using the mask dimensions the positions of the other 8 sets of peaks were calculated. With the known peak locations the image was split into separate images containing only the data from peaks of the same breakthrough energy. The space between each of the spatial samples for each image was then interpolated to

build a beam profile for each of the 9 energies.

FIG. 2 A) shows the raw image captured from the rear of the Lanex. In FIG. 2 B) the peak locations for the lowest energy peak are mapped to the image. By translating this grid by multiples of the step separation the locations of all the peaks of each of the 9 energies can be located. This process only needs to be completed once to create maps of the peak locations, which should be consistent shot to shot, allowing for improved analysis efficiency. Once the peaks of a given energy are located the raw image can be sampled at each of the peak locations and the data between the peak samples can be interpolated to retrieve the spatial profile of the beam for the given proton energy. In FIG. 2 C) the 9 interpolated beam profiles corresponding to the 9 minimum breakthrough energies are displayed. A proton spectrum can then be obtained by summing the signal across each of the interpolated profiles, as shown in FIG. 3 in blue. Significant signal is seen on the first 3 energy bins (the top row in FIG. 2 C), covering 1.1 MeV to 6.0 MeV) with some minor signal obscured by the slit in bin 4 (8.1 MeV). Removal of the slit may reveal more signal, as the proton beam is expected to be less divergent and thus a smaller size at higher proton energies.

Work is required to differentiate the proton signal from signal caused by electrons and X-rays emitted from the target rear. Due to the Bragg profile of the protons the majority of the signal measured from the scintillator is expected to be protons however a background signal will be caused by these electrons and X-rays. One proposed analysis method to distinguish protons is to consider the region of the spectrum where the signal is roughly flat as signal due to electrons and X-rays. From this a region a linear spectrum of non-proton noise is extrapolated and subtracted from the whole spectrum as show in red in FIG. 3, with the resulting subtracted spectrum shown in green. This assumption is made on the basis that MeV scale electrons and X-rays will deposit a minimal amount of energy in the 350 um thick Lanex compared with the protons depositing energy through the Bragg peak. Rigorous testing with a known proton source will be required to confirm this and also complete an absolute flux calibration.

5 Conclusion

In summary, we present a version under development of the LLNL PROBIES device. Our mask was 3D printed on-site using CLF expertise and tested in the Gemini TA3 target area. Using the device, the spectrum of a laser-driven proton source was measured over a range of 1 - 20 MeV during an experiment completing over 1200 shots on solid targets. At present the readout time of the CCD and the computational load of the 9 interpolations limits the shot rate of the device, however With optimisation of the image capture and analysis methods the device will be able to operate at the Hz level. Simple alteration of the mask design allows adjustment of the spatial and spectral resolution, although the two are inherently coupled. Splitting the spatial samples and interpolating the images allows a basic reconstruction of the spatial profile of each of the proton energies sampled in the beam. The flat signal in the high-energy bins was used to estimate the contribution from electrons and X-rays, however further work will be required to verify this and complete an absolute flux calibration. The device was operated with a simple fibre-bundle imaging setup, allowing the CCD to be located off-axis and outside of the target chamber. Additional effort will realise this device as a high-repetition tool for proton measurement.

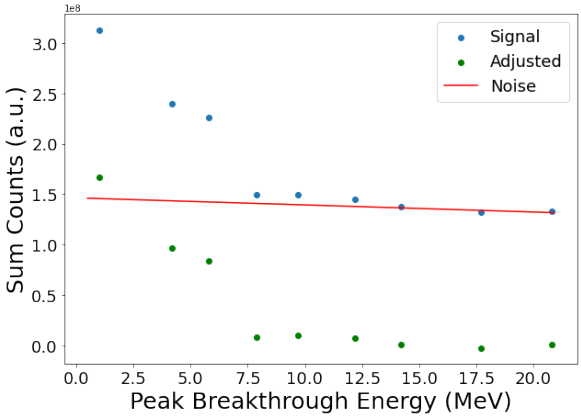

Figure 3: The raw spectrum (blue) measured by the device. A linear fit (red) using the nearly flat regions of signal at the higher energy bin was used as an approximation of electron and X-ray noise. The spectrum with this noise contribution removed is shown in green.

References

[1] R. Shalloo *et al* 2020 *Nat Commun* **11** 6355
[2] B. Loughran *et al* 2023 *Manuscript Under Review*
[3] A. Higginson *et al* 2018 *Nat Commun* **9** 724
[4] J. Green *et al* 2011 *Proc. SPIE* **807919**
[5] D. Mariscal *et al* 2021 *Plasma Phys. Control. Fusion* **63** 114003
[6] D. Mariscal *et al* 2023 *Rev. Sci. Instrum.* **94** 023507
[7] N. Xu *et al* 2023 *HPSLE* **11** e23
[8] R. A. Snavely *et al* 2000 *Phys. Rev. Let.* **85** 14